Available online at www.sciencedirect.com
ScienceDirect
Trans. Nonferrous Met. Soc. China 21(2011) 388−394

Transactions of Nonferrous Metals Society of China
www.tnmsc.cn

First-principles calculation of structural and elastic properties of $Pd_{3-x}Rh_xV$ alloys

WANG Tao-fen[1, 2], CHEN Ping[1], DENG Yong-he[1], TANG Bi-yu[1]

1. Key Laboratory of Low Dimensional Materials and Application Technology of Ministry of Education,
Department of Physics, Xiangtan University, Xiangtan 411105, China;
2. Department of Physics, Hunan University of Science and Technology, Xiangtan 411201, China

Received 20 March 2010; accepted 15 July 2010

Abstract: The structural stability, electronic and elastic properties of $Pd_{3-x}Rh_xV$ alloys with $L1_2$ and $D0_{22}$ structures were investigated theoretically by the first-principles calculations. The results reveal that with the increase of Rh content, the unit cell volume of $Pd_{3-x}Rh_xV$ alloys with $L1_2$ and $D0_{22}$ structures decreases, and the structure of $Pd_{3-x}Rh_xV$ alloys tends to transform from $D0_{22}$ to $L1_2$. The elastic parameters such as elastic constants, bulk modulus, shear modulus, elastic modulus, and Poisson ratio, were calculated and discussed in details. Electronic structures were also computed to reveal the underlying mechanism for the stability and elastic properties.

Key words: $Pd_{3-x}Rh_xV$ alloys; first-principle calculations; electronic structure; elastic properties

---

1 Introduction

The transition metals and their inter-metallic alloys are promising structural materials because of their high melting points, high strength, and good oxidation resistances[1]. In recent years, the inter-metallic alloys have attracted considerable experimental and theoretical interests of many researchers[2]. Experimental results on many inter-metallic alloys reveal that the $L1_2$ atomic order is significantly more ductile than the $D0_{22}$ order, due to the lack of a sufficient number of slip systems in the $D0_{22}$ structure[3]. Consequently, the $L1_2$ alloys are more suitable in structural applications because of their excellent mechanical properties[4]. Whereas the $D0_{22}$ structure is an ordered tetragonal phase and closely related to the $L1_2$ structure (by a 1/2 [110] shift on every (001) plane). Through part replacement of high e/atom atoms in $D0_{22}$-based alloys with low e/atom atoms, the $D0_{22}$-based alloys can be transformed into the $L1_2$ structure[5]. Therefore, it is expected that the mechanical properties of these modified $D0_{22}$-based alloys can be improved because of the availability of more slip systems in the $L1_2$ structure[6].

Recent studies proved that it is possible to modify the microstructure of $D0_{22}$. For example, LIU[7] found that although Ni_3V compound is prone to crystallize into the tetragonal $D0_{22}$ structure. by adding Co and Fe into Ni_3V, the pseudobinary compound $(Ni, Co, Fe)_3V$ can be stabilized either in the cubic $L1_2$ structure or in the tetragonal $D0_{22}$ structure, depending on the Co or Fe content. The reason is that Co or Fe has lower e/atom than Ni, so the addition of Co or Fe to Ni_3V can lower the overall e/atom to an appropriate value. In addition, similar experimental study was performed for Pd_3V and Rh_3V compounds[8]. It was found that the Pd_3V alloys are prone to crystallize into the tetragonal $D0_{22}$ structure, while the Rh_3V alloys prefer to $L1_2$ structure[8−9]. Hence, it is expected that substituting Pd by Rh can stabilize the $L1_2$ structure and further improve the mechanical properties of Pd_3V-based compounds.

Nowadays, *ab initio* calculations are extensively

Foundation item: Project (50861002) supported by the National Natural Science Foundation of China; Project (0991051) supported by the Natural Science Foundation of Guangxi Province, China; Project (08JJ6001) supported by the Natural Science Foundation of Hunan Province, China; Project (KF0803) supported by Key Laboratory of Materials Design and Preparation Technology of Hunan Province, China; Project (X071117) supported by the Scientific Research Foundation of Guangxi University, China

Corresponding author: TANG Bi-yu; Tel: +86-13187321190; E-mail: tangbiyu@xtu.edu.cn

DOI: 10.1016/S1003-6326(11)60726-7

used to predict the structure, stability and mechanical properties of pseudobinary alloys[10]. In order to get a better understanding of structural stability and mechanical properties of $Pd_{3-x}Rh_xV$ alloys after the substitution of Pd with Rh in Pd_3V alloys, *ab initio* theoretical calculations of $Pd_{3-x}Rh_xV$ inter-metallic compounds are necessary. The main aim of this study is to investigate the effect of substitution of Pd with Rh on the structural stability and mechanical properties, and provide valuable theoretical results to optimize and design the transition metal alloys.

2 Method of calculation

All calculations were done by using the Vienna *ab-initio* Simulation Package (VASP) program[11], which is based on density functional theory (DFT). The Perdew–Wang (PW91) version of the generalized gradient approximation (GGA)[12] was used to describe the exchange correlation function, and the projector augmented wave (PAW) method[13] was used in the present work. The cutoff energy (E_{cut}) of atomic wave functions was set at 350 eV. The Brillouin zone integrations used Monkhorst–Pack grids [14] of 12×12×12 for $L1_2$ and 12×12×8 for $D0_{22}$, respectively. The *k*-point was increased to 18×18×18 ($L1_2$) and 18×18×12 ($D0_{22}$) for the density of states (DOS) calculation. Atomic geometry optimization was performed by full relaxation with the conjugate gradient method until the total energy changes within 10^{-5} eV/atom and the Hellmann-Feynman force on all atomic sites was than 10^{-2} eV/Å. The first-order Methfessel-Paxton[15] method with a width of 0.2 eV was used for total energy calculations, and the calculations of density of states (DOS) were performed with the linear tetrahedron method with Bloch correction[16−17]. The elastic constants were obtained by calculating the total energy as a function of appropriate lattice deformation[18].

3 Results and discussion

3.1 Structural parameters

The structural optimization was firstly performed with the conjugate-gradient algorithm by full relaxation of unit cell volume and shape as well as the internal atomic positions. The equilibrium lattice constants were obtained from the minimum total energy. The lattice parameters for pure Pd, Rh, V and $Pd_{3-x}Rh_xV$ are reported in Table 1, together with the experimental and other theoretical results in Refs.[19−23]. For pure metal Pd, Rh, V, and alloys Pd_3V ($D0_{22}$) and Rh_3V ($L1_2$), the calculated values of lattice constants are in good agreement with the experimental values, implying that the calculation parameters chosen in this work are valid. In addition, it is noticeable that as the Rh content increases, the unit cell volume of $Pd_{3-x}Rh_xV$ decreases in both the $L1_2$ and $D0_{22}$ structures. Therefore, it can be concluded that the substitution of Pd with Rh leads to the contraction of $Pd_{3-x}Rh_xV$ alloy in both $L1_2$ and $D0_{22}$ structures.

Table 1 Calculated lattice constants, equilibrium volume *V* together with available experimental data

System	Calculated data			Experimental data
	a/Å	*c*/Å	*V*/Å^3	*a*/Å
Pure-Pd(fcc)	3.948			3.889[19]
Pure-Rh(fcc)	3.840			3.802[20]
Pure-V(bcc)	2.977			3.038[21]
$Pd_3V(L1_2)$	3.889	3.889	58.818	
$Pd_3V(D0_{22})$	3.872	7.817	117.195	3.847[22]
$Pd_2RhV(L1_2)$	3.813	3.953	57.473	
$Pd_2RhV(D0_{22})$	3.891	7.633	115.563	
$PdRh_2V(L1_2)$	3.870	3.750	56.163	
$PdRh_2V(D0_{22})$	3.828	7.724	113.184	
$Rh_3V(L1_2)$	3.805	3.805	55.089	3.784[23]
$Rh_3V(D0_{22})$	3.822	7.576	110.668	

3.2 Formation heat and cohesive energy

For the better understanding of the stability of $Pd_{3-x}Rh_xV$ alloys, the calculation of formation heat and cohesive energy was performed[24]. The average formation heat of $Pd_{3-x}Rh_xV$ alloy is defined as[25]:

$$\Delta\overline{H}=\frac{1}{x+y+z}(E_{\text{tot}}-xE_{\text{solid}}^{\text{pd}}-yE_{\text{solid}}^{\text{Rh}}-zE_{\text{solid}}^{\text{V}}) \quad (1)$$

where $\Delta\overline{H}$ is the average formation heat per atom; E_{tot} is the total energy of the unit cell; $E_{\text{solid}}^{\text{Pd}}$, $E_{\text{solid}}^{\text{Rh}}$ and $E_{\text{solid}}^{\text{V}}$ are the energy per atom of bulk Pd, Rh and V, respectively; *x*, *y* and *z* refer to the numbers of Pd, Rh and V atoms in unit cell.

The obtained formation heat of $Pd_{3-x}Rh_xV$ is shown in Fig.1. From Fig.1, it is found that for $L1_2$ structure, the negative formation heat of $Pd_{3-x}Rh_xV$ becomes lower when *x* increases from 0 to 3, so the $Pd_{3-x}Rh_xV$ alloys become more stable from the energetic point of view. While for the $D0_{22}$ structure, with the increase of *x*, the formation heat of $Pd_{3-x}Rh_xV$ is also smaller, indicating that the addition of Rh component in binary alloys (Pd_3V) also increases the stability of $D0_{22}$ crystal structure. In addition, it should be noted that when *x* is equal to 0 or 1，the heat formation of $D0_{22}$ structure is more negative than that of $L1_2$ structure, so the Pd_3V and Pd_2RhV are prone to $D0_{22}$ structure. When *x* is 2 or 3, the heat

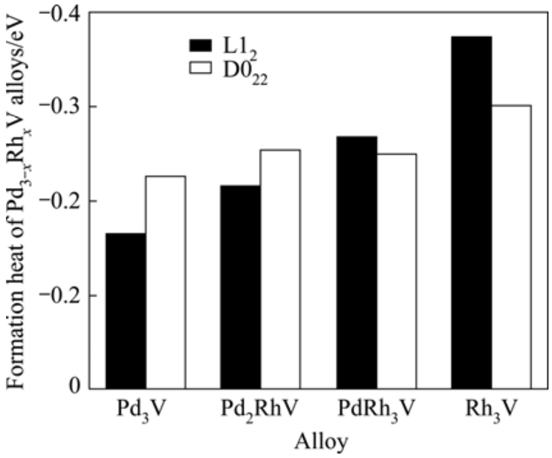

Fig.1 Formation heat of $Pd_{3\text{-}x}Rh_xV$ alloys

formation of $L1_2$ structure is more negative than that of $D0_{22}$, hence, the $PdRh_2V$ and Rh_3V show the preference to $L1_2$ structure. Therefore, with the increase of x, the crystal structure of $Pd_{3\text{-}x}Rh_xV$ possesses the transformation tendency from the $D0_{22}$ to $L1_2$ structure, which can improve the mechanic properties of the $Pd_{3\text{-}x}Rh_xV$.

The stability of crystal structure is also correlated to its cohesive energy[26], and the cohesive energy is often defined as energy needed when crystal is decomposed into the single atom. Generally, the lower the cohesive energy is, the more stable the crystal structure is[27]. In this work, the average cohesive energy is calculated with the following formula[28]:

$$E_{\text{coh}} = \frac{1}{(x+y+z)}(E_{\text{tot}} - xE_{\text{atom}}^{\text{Pd}} - yE_{\text{atom}}^{\text{Rh}} - zE_{\text{atom}}^{\text{V}}) \quad (2)$$

where E_{tot} is the electronic total energy of $Pd_{3\text{-}x}Rh_xV$ unit cell; x, y and z are the numbers of Pd, Rh and V atoms in unit cell of $Pd_{3-x}Rh_xV$ alloy, respectively; $E_{\text{atom}}^{\text{Pd}}$, $E_{\text{atom}}^{\text{Rh}}$ and $E_{\text{atom}}^{\text{V}}$ are the electronic total energies of single Pd, Rh and V atom in freedom state.

The obtained cohesive energy of $Pd_{3-x}Rh_xV$ is listed in Table 2. From Table 2, it is found that for $L1_2$ structure, the cohesive energy of $Pd_{3-x}Rh_xV$ becomes lower when x changes from 0 to 3, so the $L1_2$ $Pd_{3-x}Rh_xV$ would be more stable. For $D0_{22}$ structure, with the increase of x, the cohesive energy of $Pd_{3-x}Rh_xV$ exhibits a similar variation tendency with that of the $L1_2$. So, $Pd_{3-x}Rh_xV$ is more stable through the substitution of Pd with Rh. From the present results, it is clear that the Pd_3V and Pd_2RhV are prone to $D0_{22}$ structure, and the $PdRh_2V$ and Rh_3V show the preference to $L1_2$ structure. The results are consistent with the formation heat analyses of $Pd_{3-x}Rh_xV$ alloys.

Hence, from the results of formation heats and cohesive energies above, it could be expected that with the increase of x, $Pd_{3-x}Rh_xV$ alloys possess the transformation tendency from $D0_{22}$ to $L1_2$ structure by substitution of Pd with Rh in binary alloys (Pd_3V), and can further improve the mechanical properties of Pd_3V compound. The reasons may be attributed to the fact that the addition of Rh with lower e/atom than Pd can lower the overall e/atom of alloys to an appropriate value.

Table 2 Cohesive energy of $Pd_{3\text{-}x}Rh_xV$ alloys

System	Cohesive energy/eV
$Pd_3V(L1_2)$	−4.319
$Pd_3V(D0_{22})$	−4.380
$Pd_2RhV(L1_2)$	−4.961
$Pd_2RhV(D0_{22})$	−4.998
$PdRh_2V(L1_2)$	−5.605
$PdRh_2V(D0_{22})$	−5.586
$Rh_3V(L1_2)$	−6.302
$Rh_3V(D0_{22})$	−6.229

3.3 Density of states (DOS)

To further reveal the underlying mechanism of the structural stability for the $Pd_{3\text{-}x}Rh_xV$ alloy, the electronic total and partial densities of states (DOS) of alloys were calculated, and the results for the $L1_2$ and $D0_{22}$ structures are shown in Fig.2 and Fig.3, respectively.

For comparison and analysis, the total and partial densities of states (DOS) of Pd, Rh and V were also calculated. From Fig.2 and Fig.3, it is seen that for both the $L1_2$ and $D0_{22}$ structures of $Pd_{3\text{-}x}Rh_xV$, the DOS is mainly dominated by d electrons of Pd, Rh and V, and the partial densities of states of Pd (s), Pd(p), Rh(s), Rh(p) and V(s), V(p) in $Pd_{3-x}Rh_xV$ alloys are much less than the d partial densities of states. Concretely speaking, from the total DOS in Fig.2(a) and Fig.3(a), it is shown that the main bonding peaks of Pd_3V for $L1_2$ and $D0_{22}$ structure in the energy range under Fermi level (about from −5.4 eV to −0.4 eV) are mainly dominated by valence electron of Pd(d) orbits, and the V(d) valence electron orbits mainly dominates the energy range (about from 0 to 0.8 eV) upon the Fermi level. By further comparison between Figs.2(b) and (c) or Fig.3(b) and (c), it is revealed that the energy range under Fermi level for both the $L1_2$ and $D0_{22}$ structures of $Pd_{3-x}Rh_xV$ (x=1, 2) is mainly affected by the valence electron of both Pd(d) and Rh(d) orbits. Moreover, with the increases of x, the effect of Rh (d) orbits is more prominent under Fermi level. In addition, the electron in low-energy region of Fermi level is related to the stability of crystal structure[14]. Hence, when x increases, the hybridization between Pd-, Rh- and V-d states under Fermi level becomes strong, and the stability of $Pd_{3-x}Rh_xV$ alloys of both $L1_2$ and $D0_{22}$ structure increases.

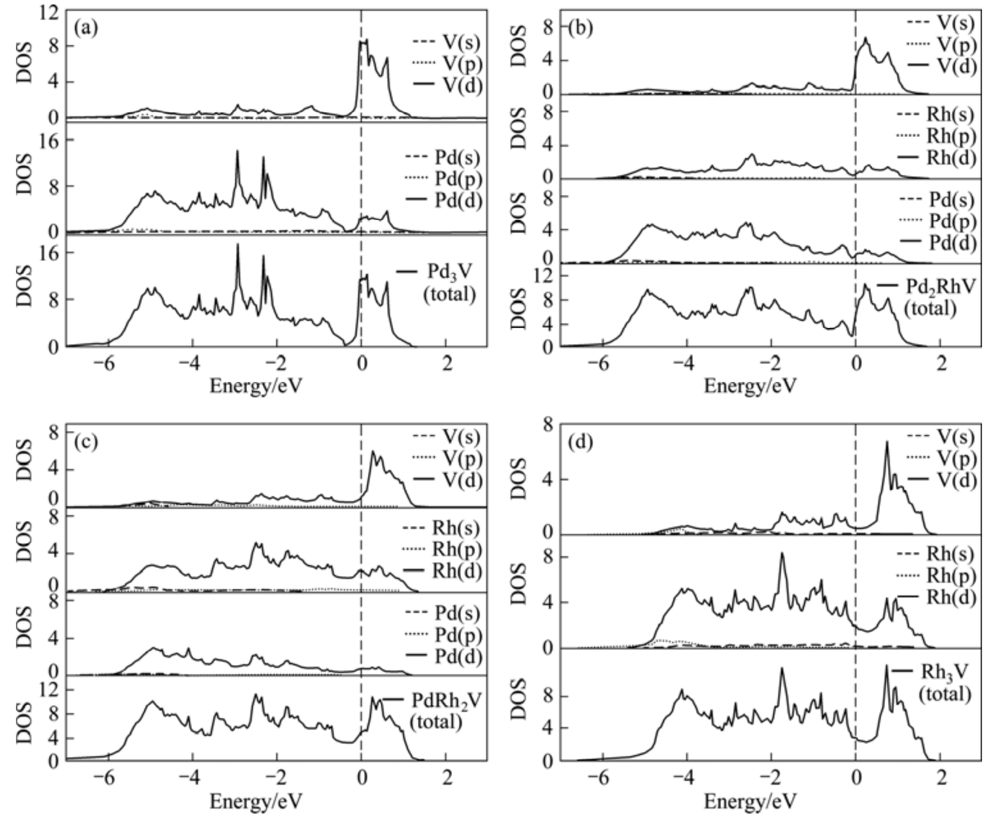

Fig.2 Partial and total densities of states of L1$_2$ structure in Pd$_{3-x}$Rh$_x$V alloys (Fermi level is set at zero energy and marked by vertical dashed lines)

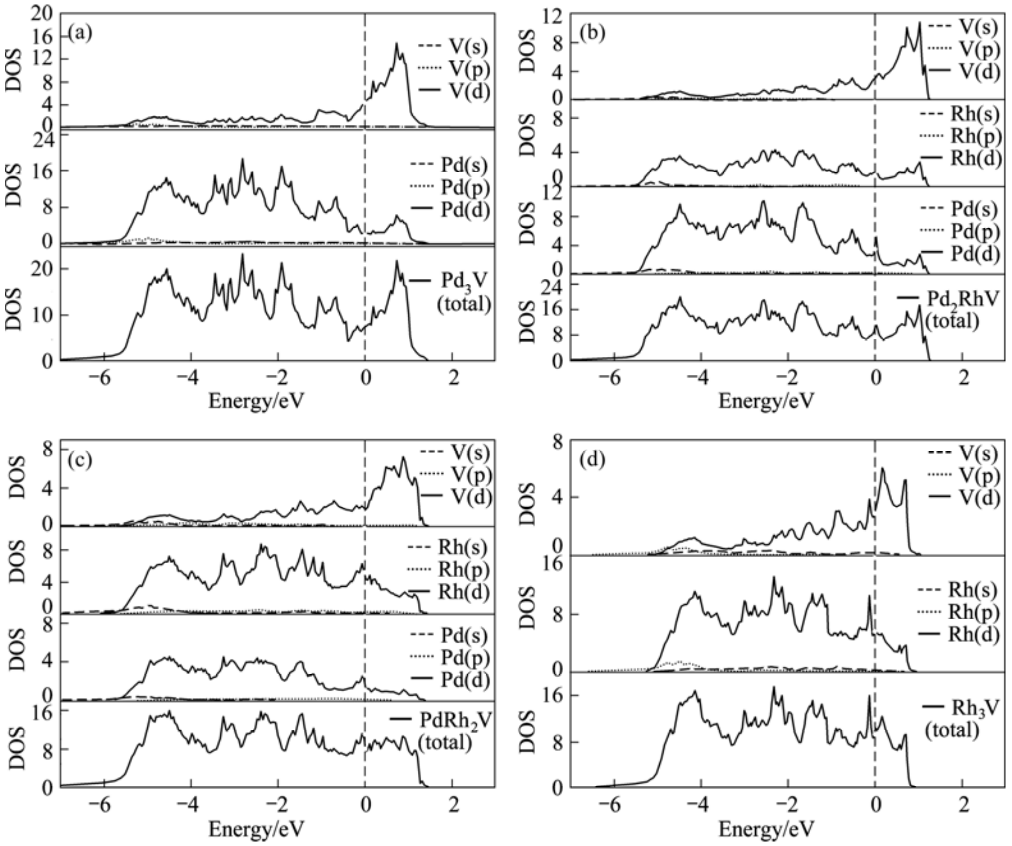

Fig.3 Partial and total densities of states of D0$_{22}$ structure in Pd$_{3-x}$Rh$_x$V (Fermi level is set at zero energy and marked by vertical dashed lines)

3.4 Elastic constants

Generally, the elastic constants are closely related to the mechanical behavior of the materials and also provide the information about the bonding characteristic. The crystal elastic constants can be obtained by the first-principles calculation of the total energy as a function of appropriate lattice deformation. For small strains, Hooke's law is valid and the crystal energy E is a quadratic function of strain. Thus, to obtain the total minimum energy for calculating the elastic constants to the second order, a crystal is strained and all the internal parameters are relaxed[29].

The calculated values of elastic constants C_{ij} are listed in Table 3. It can be seen from Table 3 that for the $Pd_{3-x}Rh_xV$ alloys with the $L1_2$ structure, all C_{ij} values become larger as x increases. While for $D0_{22}$ structure, the C_{12} and C_{66} increase as x increases, implying that the Rh component shows much more effects on the two directions. In addition, for the $Pd_{3-x}Rh_xV$ alloys in the $L1_2$ and $D0_{22}$ structures, the elastic constant C_{33} is larger than C_{11}, showing that the incompressibility along ⟨001⟩ is larger than that along ⟨100⟩, and the atomic bonding along ⟨001⟩ is also stronger than that along ⟨100⟩.

The requirement of mechanical stability for cubic crystals leads to the following restrictions on the elastic constants[30]:

$$C_{11}-C_{12}>0,\quad C_{11}+2C_{12}>0,\quad C_{11}>0,\quad C_{44}>0 \tag{3}$$

And the mechanical stability criteria for tetragonal crystals are[29]

$$C_{11}-C_{12}>0,\ C_{11}+C_{33}-2C_{13}>0,\ 2C_{11}+C_{33}+2C_{12}+4C_{13}>0,\ C_{11}>0,\ C_{33}>0,\ C_{44}>0,\ C_{66}>0 \tag{4}$$

The calculated elastic constants of $Pd_{3-x}Rh_xV$ alloy in $L1_2$ and $D0_{22}$ structures are in good agreement with the above criteria, indicating that all of them are mechanically stable.

Based on the single-crystal elastic constants, the polycrystalline elastic modulus is also estimated by the Voigt-Reuss-Hill (VRH) approximation[31]. For the cubic structure[32], the bulk modulus K, shear modulus G, elastic modulus E, and Poisson ratio (v) are calculated as follows:

$$K=(C_{11}+2C_{12})/3 \tag{5}$$

$$G_V=(C_{11}-C_{12}+3C_{44})/5 \tag{6}$$

$$G_R=5(C_{11}-C_{12})C_{44}/[4C_{44}+3(C_{11}-C_{12})] \tag{7}$$

$$G=(G_V+G_R)/2 \tag{8}$$

$$E=9GK/(3K+G) \tag{9}$$

$$v=(E-2G)/2G \tag{10}$$

For the tetragonal lattice, the equations are[31]

$$K=[(C_{11}+C_{12})C_{33}-2C_{13}^2]/(C_{11}+C_{12}+2C_{33}-4C_{13}) \tag{11}$$

$$G_V=(2C_{11}+C_{33}-C_{12}-2C_{13}+6C_{44}+3C_{66})/15 \tag{12}$$

$$G_R=15/(8s_{11}+4s_{33}-4s_{12}-8s_{13}+6s_{44}+3s_{66}) \tag{13}$$

where s_{ij} are the compliance constants.

$$s_{11}+s_{12}=C_{33}/C,\ s_{11}-s_{12}=1/(C_{11}-C_{12}),\ s_{13}=-C_{13}/C,\ s_{33}=(C_{11}+C_{12})/C,\ s_{44}=1/C_{44},\ s_{66}=1/C_{66};\ G=(G_V+G_R)/2;\ E=9GK/(3K+G);\ v=(E-2G)/2G;\ C=C_{33}(C_{11}+C_{12})-2C_{13}^2 \tag{14}$$

The calculated polycrystalline elastic modulus are listed in Table 4. In general, the elastic modulus can effectively describe the elastic properties of $Pd_{3-x}Rh_xV$ alloys. The bulk modulus K is a measure of resistance to volume change by applied pressure and the shear modulus G is a measure of resistance to reversible deformations upon shear stress[33]. The larger the K and G are, the higher the resistances to volume change and reversible shear deformations are. The elastic modulus E is used to provide a measure of stiffness of the solid. The larger the elastic modulus is, the stiffer the material is[34]. Table 4 shows that with increasing x, the calculated bulk modulus K, shear modulus G and elastic

Table 3 Crystal elastic constants for $L1_2$ and $D0_{22}$ in compounds

Compound	C_{11}/GPa	C_{12}/GPa	C_{13}/GPa	C_{33}/GPa	C_{44}/GPa	C_{66}/GPa
$Pd_3V(L1_2)$	265.287	156.456			88.383	
$Pd_3V(D0_{22})$	247.535	181.356	159.574	274.877	106.034	117.995
$Pd_2RhV(L1_2)$	303.910	173.780	162.023	304.682	122.529	131.807
$Pd_2RhV(D0_{22})$	239.138	181.528	150.688	266.728	102.591	129.796
$PdRh_2V\ (L1_2)$	348.813	171.440	179.124	350.183	144.468	147.659
$PdRh_2V\ (D0_{22})$	303.551	202.302	166.560	316.177	123.636	141.923
$Rh_3V(L1_2)$	410.081	181.407			199.039	
$Rh_3V(D0_{22})$	354.850	217.355	184.238	396.653	168.801	160.535

Table 4 Constants of $Pd_{3-x}Rh_xV$

Compound	K/GPa	G/GPa	E/GPa	v
$Pd_3V(L1_2)$	192.733	72.760	193.882	0.332
$Pd_3V(D0_{22})$	196.753	75.237	200.194	0.330
$Pd_2RhV(L1_2)$	211.956	98.722	256.365	0.298
$Pd_2RhV(D0_{22})$	190.084	73.883	196.226	0.328
$PdRh_2V$ $(L1_2)$	234.096	118.014	303.106	0.284
$PdRh_2V$ $(D0_{22})$	221.318	96.729	253.286	0.309
$Rh_3V(L1_2)$	257.632	159.350	396.335	0.244
$Rh_3V(D0_{22})$	253.086	126.448	325.187	0.286

modulus E of $L1_2$ $Pd_{3-x}Rh_xV$ alloys increase. On the other hand, the Poisson ratio is used to quantify the stability of the crystal against shear, which usually ranges from −1 to 0.5. All the calculated Poisson ratios of $Pd_{3-x}Rh_xV$ $(L1_2)$ alloys do not exceed 0.35, which means that with increasing x, $Pd_{3-x}Rh_xV$ alloys still possess good stability against shear. Obviously, the overall elastic properties of $Pd_{3-x}Rh_xV$ $(L1_2)$ alloys have been improved with increasing x, which is consistent with the results of LIU[7]. In contrary, for the $Pd_{3-x}Rh_xV$ $(D0_{22})$ alloys, the elastic modulus does not increase monotonously with increasing x. As seen in Table 4, the elastic modulus of the Pd_2RhV $(D0_{22})$ is lower than that of Pd_3V, while the elastic modulus of the $PdRh_2V$ $(D0_{22})$ is higher than that of Pd_3V. In addition, it can be easily found that K, G and E of $Pd_{3-x}Rh_xV$ $(L1_2)$ alloys are superior to those of the $D0_{22}$-based alloys with the same x, indicating that the substitution of Pd with Rh is an effective way to improve the elastic properties. Up to now, there is still no report on experimental values of these parameters, so the above theoretical results obtained here provide a reference for the future experimental work.

4 Conclusions

1) The structural stability and elastic properties of $Pd_{3-x}Rh_xV$ alloys in $L1_2$ and $D0_{22}$ structures were investigated based on density-functional theory (DFT) with the generalized gradient approximation (GGA).

2) The results show that the substitution of Pd with Rh leads to contraction of the lattice of $Pd_{3-x}Rh_xV$ alloys. Furthermore, with the increase of x, $L1_2$ crystal structure becomes more stable and the $Pd_{3-x}Rh_xV$ tends to transform from the $D0_{22}$ to $L1_2$ structure, although the substitution of Pd with Rh in binary alloys Pd_3V can result in the stable formation of $Pd_{3-x}Rh_xV$ alloys of both $L1_2$ and $D0_{22}$ crystal structure.

3) The calculated electronic structure shows that the hybridization between Rh-d states and V-d states can stabilize $L1_2$- and $D0_{22}$-$Pd_{3-x}Rh_xV$. In addition, the present investigations show that the elastic properties of $L1_2$-based $Pd_{3-x}Rh_xV$ alloys are improved with the increase of x. In contrary, for $Pd_{3-x}Rh_xV$ alloys with the $D0_{22}$ structure, the elastic modulus of Pd_2RhV decreases, while elastic parameters for $PdRh_2V$ increase.

References

[1] COLINET C, PASTUREL A. Phase stability and electronic structure of the $HfAl_3$ compound [J]. Phys Rev B, 2001, 64: 205102.

[2] LEBACQ O, PASTUREL A, MANH D N, FINEL A, CAUDRON R. Electronic structure, cohesive properties and phase stability in Ni_3V, Pd_3V, and Pt_3V compounds [J]. J Alloys Compd, 1998, 264: 31−37.

[3] PETTIFOR D G, COTTRELL A H. Electron theory in alloy design [M]. London: The Institute of Materials, 1992: 158.

[4] SINHA A K. Close-packed ordered ABs structures in ternary alloys of certain transition metals [J]. Trans AIME, 1969, 245: 911−917.

[5] TIAN W H, NEMOTO M. Morphology of $L1_0$-TiAl(Ag) precipitation in Ag-modified $L1_2$-Al_3Ti [J]. Intermetallics, 2000, 8: 345−352.

[6] MORRIS D G, MORRIS M A. The stress anomaly in FeAl-Fe_3Al alloys[J]. Intermetallics, 2005, 13: 1269−1274.

[7] LIU C T. Physical metallurgy and mechanical properties of ductile ordered alloys (Fe, Co, Ni) V [J]. Intl Met Rev, 1984, 29: 168−194.

[8] LOISEAU A, CABET E. $L1_2D0_{22}$ competition in the pseudo binary (Pt, $Rh)_3V$ and (Pd, $Rh)_3V$ alloys[J]. J Physique IV, 1993, 3: C7−2051.

[9] CABET E, PASTUREL A, DUCASTELLE F, LOISEAU A. $L1_2$-DO_{22} competition in the pseudobinary (Pt, $Rh)_3V$, Pt_3(V, Ti), and (Pd, $Rh)_3V$ alloys: Phase stability and electronic structure[J]. Phys Rev Lett, 1996, 76: 3140−3143.

[10] COLINET C, PASTURE A. Theoretical calculation of the phase diagram between one-dimensional long-period structures in the quasi binary sections: $Pd_{3x}Rh_{3(1-x)}V$, $Pt_{3x}Rh_{3(1-x)}V$, and $Pt_3V_xTi_{(1-x)}$ [J]. Calphad, 2002, 26: 563−571.

[11] KRESSE G, FURETHMÜLLER J. Efficient iterative schemes for *ab initio* total-energy calculations using a plane-wave basis set[J]. Phys Rev B, 1996, 54: 11169−11186.

[12] PERDEW J P, CHEVARY J A, VOSKO S H. Atoms, molecules, solids, and surfaces: Applications of the generalized gradient approximation for exchange and correlation [J]. Phys Rev B, 1992, 46: 6671−6687.

[13] BLOCHL P E. Projector augmented-wave method [J]. Phys Rev B,

1994, 50: 17953−17979.

[14] DENG Yong-he, WANGT Tao-fen, ZHANG Wei-bing, TANG Bi-yu, ZHNG Xiao-qin, DING Wen-jiang. Crystal structure investigation of Mg$_3$Pd from first-principles calculations[J]. Transactions of Nonferrous Metals Society of China, 2008, 18(2): 41−45.

[15] METHFESSEL M, PAXTON A T. High-precision sampling for Brillouin-zone integration in metals [J]. Phys Rev B, 1989, 40: 3616−3621.

[16] BLOCHL P E, JEPSEN O, ANDERSEN O K. Improved tetrahedron method for Brillouin-zone integrations [J]. Phys Rev B, 1994, 49: 16223−16233.

[17] TANG B Y, WANG N, YU W Y. Theoretical investigation of typical fcc precipitates in Mg-based alloys [J]. Acta Materialia, 2008, 56: 3353−3357.

[18] WALLACE D C, Thermodynamics of crystals [M]. New York: Wiley, 1972: 106−120.

[19] LAWSON A C, CONANT J W, ROBERTSON R. Debye-Waller factors of PdD$_x$ materials by neutron powder diffraction[J]. J Alloys Compd, 1992, 183: 174−180.

[20] ELLNER M, KOLATSCHEK K, PREDEL B. On the partial atomic volume and the partial molar enthalpy of aluminium in some phases with Cu and Cu$_3$Au structures [J]. Journal of the Less-Common Metals, 1991, 170: 171−184.

[21] KORLING M, HAGLUNG J. Cohesive and electronic properties of transition metals: The generalized gradient approximation[J]. Phys Rev B, 1992, 45: 13293−13297.

[22] DWIGHT A E, DOWNEY J W, CONNER R A. Some AB$_3$ compounds of the transition metals [J]. Acta Crystallographica, 1961, 14: 75−76.

[23] WATERSTRAT R M, MANUSZEWSKI R C. The vanadium-rhodium constitution diagram [J]. Journal of the Less-Common Metals, 1977, 52: 293−305.

[24] SONG Y, GUO Z X, YANG R. Influence of selected alloying elements on the stability of magnesium dihydride for hydrogen storage applications: A first-principles investigation[J]. Phys Rev B, 2004, 69(9): 094205.

[25] ZUBOV V I, SANCHEZ J F, TEIXEIRA J N. Theoretical study of the saturated vapor pressure and enthalpy of sublimation of C$_{60}$ sfullerite [J]. Phys Lett B, 1997, 55: 6747−6749.

[26] MASSARD R, UZIO D, THOMAZEAU C. Strained Pd overlayers on Ni nanoparticles supported on alumina and catalytic activity for buta-1, 3-dience selective hydrogenation [J]. J Catalysis, 2007, 245: 133−143.

[27] GHOSH G. First-principles calculations of structural energetics of Cu-TM(TM=Ti, Zr, Hf) intermetallics [J]. Acta Materialia, 2007, 55: 3347−3374.

[28] ZUBOV V I, TRETIAKOV N P, TEIXEIRA J N, SANCHEZ J F. Calculations of the thermal expansion, cohesive energy and thermodynamic stability of a van der Waals crystal—fullerene C$_{60}$ [J]. Phys Lett A, 1994, 194: 223−227.

[29] PATIL S K R, KHARE S V, TUTTLE B R, BORDING J K, KODAMBAKA S. Mechanical stability of possible structures of PtN investigated using first-principles calculations [J]. Phys Rev B, 2006, 73: 104118.

[30] MATTESINI M, AHUJA R, JOHANSSON B. Cibic Hf$_3$N$_4$ and Zr$_3$N$_4$: A class of hard materials[J]. Phys Rev B, 2003, 68: 184108.

[31] HILL R. The elastic behaviour of a crystalline aggregate [J]. Proc Phys Soc A, 1952, 65: 349−354.

[32] MEHL M J, OSBURN J E, PAPACONSTANTOPOULOS D A, KLEIN B M. Structural properties of ordered high-melting -temperature intermetallic alloys from first-principles total-energy calculations [J]. Phys Rev B, 1990, 41: 10311−10323.

[33] YOUNG A F, SANLOUP C, GREGORYANZ E, SCANDOLO S, HEMLEY R J, MAO H K. Synthesis of novel transitions metal nitrides IrN$_2$ and OsN$_2$ [J]. Phys Rev Lett, 2006, 96: 155501.

[34] MATTESINI M, SOLER J M, YNDURAIN F. *A*b *initio* study of metal-organic framework-5 Zn$_4$O(1, 4-benzenedicarboxylate)$_3$: An assessment of mechanical and spectroscopic properties [J]. Phys Rev B, 2003, 73: 094111.

Pd$_{3-x}$Rh$_x$V 合金的结构和弹性性能的第一性原理计算

王桃芬 [1,2], 陈 平 [1], 邓永和 [1], 唐壁玉 [1]

1. 湘潭大学 物理系, 低维材料及其应用技术教育部重点实验室, 湘潭 411105;
2. 湖南科技大学 物理系, 湘潭 411201

摘 要：利用第一性原理对 Pd$_{3-x}$Rh$_x$V 合金的 2 种结构(L1$_2$ 和 D0$_{22}$)的相对稳定性、电子特性以及弹性性能等方面进行研究。计算结果表明：随着铑含量的增加，L1$_2$ 和 D0$_{22}$ 型结构的合金晶胞体积均减小，晶胞有一定程度的压缩。与 Pd$_3$V 相比，加入铑元素，有利于 Pd$_{3-x}$Rh$_x$V 合金的 2 种结构的稳定，并且合金结构趋于从 D0$_{22}$ 型转化为更加稳定的 L1$_2$ 型。对合金电子结构(态密度)的计算和分析说明，随着铑的加入，在费米能级以下铑和钒的杂化作用越来越明显，进一步影响 L1$_2$ 和 D0$_{22}$ 结构的稳定性。还对 Pd$_{3-x}$Rh$_x$V 合金的 L1$_2$ 和 D0$_{22}$ 结构的弹性常数，如体积模量(B)、剪切模量(G)、弹性模量(E)和泊松比(ν)等随着铑加入的变化规律进行计算和讨论。

关键词：Pd$_{3-x}$Rh$_x$V 合金；第一性原理计算；电子结构；弹性性能

(Edited by YANG Hua)